


Article

# The Use of Low-Altitude UAV Imagery to Assess Western Juniper Density and Canopy Cover in Treated and Untreated Stands

Nicole Durfee <sup>1,\*</sup>, Carlos G. Ochoa <sup>2</sup>  and Ricardo Mata-Gonzalez <sup>3</sup><sup>1</sup> Water Resources Graduate Program—Ecohydrology Lab, Oregon State University, Corvallis, OR 97331, USA<sup>2</sup> Department of Animal and Rangeland Sciences—Ecohydrology Lab, Oregon State University, Corvallis, OR 97331, USA; Carlos.Ochoa@oregonstate.edu<sup>3</sup> Department of Animal and Rangeland Sciences, Oregon State University, Corvallis, OR 97331, USA; ricardo.matagonzalez@oregonstate.edu

\* Correspondence: durfeen@oregonstate.edu; Tel.: +1-541-737-0933

Received: 12 March 2019; Accepted: 25 March 2019; Published: 29 March 2019



**Abstract:** Monitoring vegetation characteristics and ground cover is crucial to determine appropriate management techniques in western juniper (*Juniperus occidentalis* Hook.) ecosystems. Remote-sensing techniques have been used to study vegetation cover; yet, few studies have applied these techniques using unmanned aerial vehicles (UAV), specifically in areas of juniper woodlands. We used ground-based data in conjunction with low-altitude UAV imagery to assess vegetation and ground cover characteristics in a paired watershed study located in central Oregon, USA. The study was comprised of a treated watershed (most juniper removed) and an untreated watershed. Research objectives were to: (1) evaluate the density and canopy cover of western juniper in a treated (juniper removed) and an untreated watershed; and, (2) assess the effectiveness of using low altitude UAV-based imagery to measure juniper-sapling population density and canopy cover. Ground-based measurements were used to assess vegetation features in each watershed and as a means to verify analysis from aerial imagery. Visual imagery (red, green, and blue wavelengths) and multispectral imagery (red, green, blue, near-infrared, and red-edge wavelengths) were captured using a quadcopter-style UAV. Canopy cover in the untreated watershed was estimated using two different methods: vegetation indices and support vector machine classification. Supervised classification was used to assess juniper sapling density and vegetation cover in the treated watershed. Results showed that vegetation indices that incorporated near-infrared reflectance values estimated canopy cover within 0.7% to 4.1% of ground-based calculations. Canopy cover estimates at the untreated watershed using supervised classification were within 0.9% to 2.3% of ground-based results. Supervised classification applied to fall imagery using multispectral bands provided the best estimates of juniper sapling density compared to imagery taken in the summer or to using visual imagery. Study results suggest that low-altitude multispectral imagery obtained using small UAV can be effectively used to assess western juniper density and canopy cover.

**Keywords:** juniper woodlands; ecohydrology; remote sensing; unmanned aerial systems; central Oregon; rangelands

## 1. Introduction

The range and density of woody plant species such as western juniper (*Juniperus occidentalis* Hook.) have substantially increased in the western United States over the last 150 years. Estimates of juniper (*Juniperus* spp.) expansion across the Great Basin range from 125% to 625% [1] and western juniper alone can be found across 3.6 million ha in the intermountain west [2]. The expansion of

western juniper in particular has arisen in two primary forms: through the encroachment of juniper into areas previously dominated by sagebrush (*Artemisia tridentata* Nutt.), and through increases in the density of juniper in areas where it was relatively sparse [3]. Historically, juniper was largely found in areas with lower fire risk [4]. Intensive grazing, reduced fire occurrence, and favorable wetter climate conditions have all been cited as reasons for the vast juniper expansion observed in the late 19th and early 20th century [3,5].

Juniper expansion is a concern in many rangeland areas as it may lead to reduced water availability for other types of vegetation. Increased juniper canopy cover has been associated with increased bare ground and decreased shrub, forb, and grass cover [6] and reductions in vegetation production and diversity [7]. Several studies [6,8–11] have addressed the impacts of juniper expansion on ecological and hydrological processes. These impacts include increased erosion and runoff [12–14] and decreased soil moisture [8] typically associated with shifts in vegetation cover [2,12,15], particularly with increased bare ground in intercanopy locations [16].

The use of ground-based techniques to assess vegetation characteristics is limited to the resources available and normally includes an aggregate of data collected at point specific locations. Remote sensing offers the ability to assess ecological features over larger temporal and spatial scales. Remote sensing has been used successfully to identify juniper expansion [17], assess shrub cover characteristics in encroached sagebrush steppe ecosystems [18], calculate canopy cover in juniper woodlands [19,20] and characterize ground cover following treatment [21]. Remote-sensing techniques using multispectral imagery (particularly near-infrared reflectance) has improved the ability to assess changes in vegetation cover [22,23].

The use of unmanned aerial vehicle (UAV)-based data collection in remote-sensing applications can be useful in western juniper research including species classification [24], soil erosion monitoring [25], and measurements of tree canopy [26,27]. Imagery captured using remote sensing can improve our ability to study juniper removal and recovery by reducing time requirements for data collection and providing greater flexibility in observation times compared to ground-based measurements alone.

Vegetation indices derived from aerial and satellite imagery can be particularly useful for vegetation identification and classification as they provide information about vegetation characteristics by analyzing specific band reflectance properties. The relationship between different spectral bands can be used to distinguish between areas of vegetation and bare soil or rock. Vegetation indices developed from remote sensing data have been used to determine gross primary production in pinyon-juniper woodlands [28].

There is a range of vegetation indices used to assess vegetation characteristics. Reflectance characteristics from multispectral imagery, particularly the near-infrared and red-edge spectral regions, have been successfully used to assess vegetation growth [29] and to identify different vegetation species [24,30]. A commonly used vegetation index, the normalized difference vegetation index (NDVI) [31], is calculated from the reflectance characteristics of the near-infrared and red bands, and indicates photosynthetic activity. NDVI has also been found to be closely related to ground-based canopy cover calculations [32]. The optimized soil adjusted vegetation index (OSAVI) has a similar formula to that of NDVI but is used to minimize the influence of soil reflectance [33], a concern in many arid and semiarid regions with high amounts of bare soil. Another example of an index potentially useful in studying western juniper is the total ratio vegetation index (TRVI) [34], which was developed to address different vegetation characteristics in arid and semiarid ecosystems (e.g., juniper woodlands).

Other techniques used in image analysis such as classification have been utilized extensively for the detection and assessment of vegetation [35–37]. Pixel-based image analysis has been used for weed detection [38] and vegetation identification in mixed plant communities [39]. The use of classification tools for image analysis has also been shown to decrease time requirements compared to manual analysis of imagery [40], particularly over large areas. In ecosystems where juniper expansion

is occurring, visual inspection of imagery alone is time-consuming and inefficient due to the typically large areas involved. By incorporating classification into analysis of UAV-based imagery, it may be possible to more efficiently monitor juniper re-establishment after removal.

This study sought to build upon UAV-based techniques and ground-based data collection to study the spatial distribution of juniper in a treated watershed where mature western juniper was eliminated in 2005 and in an untreated watershed. Study objectives were to: (1) evaluate the density and canopy cover of western juniper in a treated (juniper removed) and an untreated watershed; and, (2) assess the effectiveness of using low altitude UAV-based imagery to measure juniper-sapling population density and canopy cover.

## 2. Materials and Methods

### 2.1. Study Site

The study was conducted at the Camp Creek Paired Watershed Study (CCPWS) site in central Oregon. The CCPWS was established in 1993 to study long-term ecohydrological relationships in western juniper-dominated landscapes [41]. The study site includes two watersheds (WS): an untreated WS (96 hectares) and a treated WS (116 hectares) (Figure 1). During 2005 to 2006, nearly 90% of western juniper trees were removed from the treated WS. Trees were cut using chainsaws, the boles were removed, and tree limbs were scattered [42].

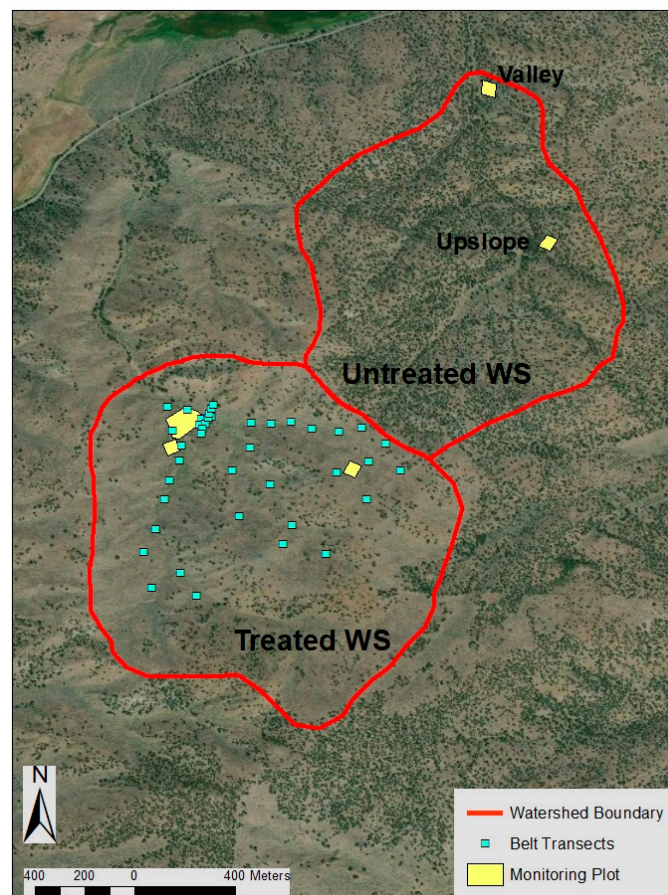


**Figure 1.** Map of the study site showing ground-based collection points and monitoring plot location in both watersheds. Study plots in the untreated watershed (WS) have been labeled to clarify position. The larger plot in the treated WS indicates the location of the unmanned aerial vehicle (UAV) imagery collection in that WS. Image created using ArcMap 10.6. Source: Esri, DigitalGlobe.

Climate in central Oregon is semiarid and precipitation falls largely during the fall and winter months. Average annual precipitation (2009–2017) at the study site is 358 mm [41]. Elevation at the study site ranges from 1350 to 1500 m. The orientation of the treated WS is primarily north by northwest while the untreated WS is largely oriented toward the north [43]. The average slope is 25% in the untreated WS and 24% in the treated WS [43].

Overstory vegetation at the treated WS is dominated by big sagebrush, while western juniper is the dominant species at the untreated WS. Understory vegetation in both watersheds is dominated by perennial grasses, primarily bluebunch wheatgrass [*Pseudoroegneria spicata* (Pursh.) Á. Löve], Idaho fescue (*Festuca idahoensis* Elmer), Indian ricegrass [*Achnatherum hymenoides* (Roem. and Schult.) Barkworth], Sandberg bluegrass (*Poa secunda* J. Presl), and Thurber's needlegrass [*Achnatherum thurberianum* (Piper) Barkworth] and some annual grasses, such as cheatgrass (*Bromus tectorum* L.) [43,44]. As reported by Ray et al. [44], juniper canopy cover at the untreated WS is 31% and at the treated WS is less than 1%, this based on surveys in 2015. According to the juniper occupancy classification described by Miller et al. [2], the untreated WS is considered at the highest level, Phase III, in which juniper is at nearly 30% occupancy and it is the dominant overstory species.

## 2.2. Vegetation Measurements

We calculated juniper-sapling population density, canopy cover, and age characteristics at the watershed scale in the treated WS, and adult and sapling-stage tree density and canopy cover at the plot scale in both watersheds.

At the watershed scale, we installed 41 belt transects (30 m by 3 m) to measure juniper-sapling count, height, and crown width in the treated WS. The belt transects were located across the landscape to represent varying aspect and slope characteristics. A subsample of 18 saplings representing common tree characteristics (i.e., height and width) observed in the treated WS were removed to determine tree age using techniques described by Phipps [45].

At the plot scale, we installed two 2000 m<sup>2</sup> monitoring plots in each watershed. One plot was installed in a valley location near the watershed outlet and one in an upstream location (Figure 1). In the untreated WS, tree canopy cover was estimated using a spherical concave densiometer (model A) (Forestry Suppliers, Jackson, MS, USA) across five 40 m parallel transects in each plot. Tree canopy cover was measured every 5 m, facing each cardinal direction, in each 40 m transect. The two plots in the untreated WS were also used to assess juniper canopy cover estimates using UAV-based imagery. All juniper (sapling and adult stages) were counted on the ground to determine tree population density in the monitoring plots at both watersheds. No adult-stage trees were present in either of the two plots in the treated WS; therefore, we only measured sapling count in each 2000 m<sup>2</sup> plot.

An 11,600 m<sup>2</sup> plot in the treated WS (Figure 1) was employed to assess juniper sapling estimates obtained using the various UAV-based methods described below. A subset of juniper saplings in the larger plot were selected to assess the accuracy of juniper identification.

## 2.3. Unmanned Aerial Vehicle (UAV)-Based Imagery Collection and Analysis

We collected UAV-based imagery from multiple low elevation (40 to 50 m) flights conducted on 21 June 2018, 15 and 16 July 2018, and 12 October 2018. In order to minimize shadows, flights occurred around noon and early afternoon. Aside from temperature, weather conditions at the time of each flight were similar with scattered clouds present and light, variable winds. Data collected in October 2018 and in the summer of 2018 were used to compare multispectral imagery results across seasons in the treated WS. Three quadcopter UAV (Table 1) were used to collect data. Multispectral imagery (red, green, blue, near-infrared, and red-edge) was captured using a RedEdge camera (MicaSense, Inc., Seattle, WA, USA). The RedEdge camera was attached either to a Matrice 100 (DJI, Shenzhen, China) or to a Solo (3D Robotics, Inc., Berkeley, CA, USA) UAV for multispectral imagery collection. RGB (red, green, and blue wavelengths) imagery was collected using a DJI Phantom 3 Professional camera (DJI, Shenzhen, China). The Phantom 3 was not used for image collection at the treated WS, the red,



green, and blue bands were extracted from the multispectral raster and used for analysis of visual imagery instead.

**Table 1.** UAVs used for data collection. Multispectral (red, green, blue, near-infrared, and red-edge bands) imagery was captured by attaching the RedEdge camera to the Solo and Matrice 100. Visual imagery (red, green, and blue bands) was collected using the Phantom 3 Professional camera.

UAV Platform	Manufacturer	Image Type
Solo	3D Robotics, Inc., Berkeley, CA, USA	Multispectral
Matrice 100	DJI, Shenzhen, China	Multispectral
Phantom 3 Professional	DJI, Shenzhen, China	Visual

These quadcopter UAV were selected for use as they provide a flexible platform that can be adapted for multiple types of data collection. Additionally, given the remote location and lack of suitable launching and landing areas, a fixed wing aircraft would be difficult to use. The quadcopters used in this study offer the advantage of being relatively easy to operate, making them an ideal candidate to be used by land managers who may not have flight experience or access to more expensive UAV.

Flight plans were created and conducted using the Pix4Dcapture (Pix4D SA, Lausanne, Switzerland) mobile application, or flown manually. Relatively low flight altitudes (40 to 50 m above ground level) were employed in order to assess the ability of the UAV-imagery to detect juniper saplings. These flight altitudes were chosen as they provide relatively high spatial resolution, while requiring less flight time than much lower flight altitudes. While time requirements for UAV-based data collection were not intensive (flights averaged less than 12 min), the intent of this study was to assess a method that could be applied to larger study areas in the future. Additionally, the height of mature juniper in the untreated WS required a minimum of 40 m flight altitude to ensure sufficient clearance from the top of the trees. An overlapping grid pattern was flown to ensure minimum 80% forward overlap and 60% side overlap. Sufficient overlap was confirmed using the PhotoScan professional (Agisoft LLC, St Petersburg, Russia) program after individual images were added and aligned. All images were captured at nadir.

Orthomosaics created using RGB imagery had slightly higher spatial resolution than those created using the multispectral imagery. Spatial resolution of the visual band orthomosaic at the untreated valley site was 2.09 cm pixel<sup>-1</sup> and 2.02 cm pixel<sup>-1</sup> at the untreated upstream site. Spatial resolution of the multispectral imagery at the untreated WS valley site was 3.15 cm pixel<sup>-1</sup> and 2.74 cm pixel<sup>-1</sup> at the untreated WS upstream site. For the multispectral imagery captured in July 2018 at the treated WS study plot, the orthomosaic was 3.00 cm pixel<sup>-1</sup>. The orthomosaic created from imagery captured in October of 2018 had a spatial resolution of 2.40 cm pixel<sup>-1</sup>.

Image processing, including the creation of orthomosaics, was conducted using PhotoScan professional (Agisoft LLC, St Petersburg, Russia). Photo alignment was performed using the highest accuracy setting, with a key point limit of 120,000 and a tie point limit of 30,000. Adaptive camera fitting was performed during this step. To create the dense cloud, the ultra-high quality setting with aggressive depth filtering was used. A mesh was created using the 2.5D height field for surface data with a high face count, using the sparse cloud. The mosaic blending mode was used to build the texture. The dense cloud was used to build the tiled model and digital elevation model (DEM). Orthomosaics were subsequently produced in PhotoScan using the created DEM. Areas with poor image quality and without sufficient overlap (on the edges of the orthomosaic) were excluded from analysis. Image analysis was conducted using ArcGIS (version 10.6, Redlands, CA, USA). No radiometric correction was performed; therefore, brightness numbers were used for image analysis. Georeferencing and alignment of images was performed in ArcGIS using landscape features (e.g., gully intersection points) and selected ground control reference markers with known latitude and longitude positions that could be easily identified in imagery.

#### 2.4. Comparative Analysis, Ground Data versus UAV Imagery

RGB imagery (red, green, and blue wavelengths) and multispectral imagery (red, green, blue, near-infrared, and red-edge wavelengths) were used to assess canopy cover and vegetation cover characteristics. Four vegetation indices were selected to assess canopy cover characteristics of the untreated study plots (Table 2). As RGB cameras are often more accessible and affordable compared to cameras that capture multispectral imagery, we assessed the effectiveness of using RGB imagery for measuring canopy cover (both mature juniper and juniper saplings), vegetation cover, and juniper identification.

**Table 2.** Vegetation indices selected to assess vegetation and ground cover characteristics of the study plots. Names refer to reflectance values for each band. The TGI uses the wavelength ( $\lambda$ ) for the red, green, and blue bands in the calculation. NIR refers to near-infrared.

Method	Formula
Triangular Greenness Index (TGI) [46]	$-0.5[(\lambda_{red} - \lambda_{blue})(Red - Green) - (\lambda_{red} - \lambda_{green})(Red - Blue)]$
Optimized Soil Adjusted Vegetation Index (OSAVI) [33]	$(NIR - Red)/(NIR + Red + 0.16)$
Normalized Difference Vegetation Index (NDVI) [31]	$(NIR - Red)/(NIR + Red)$
Total Ratio Vegetation Index (TRVI) [34]	$4[(NIR - Red)/(NIR + Red + Green + Blue)]$

In order to measure canopy cover, the triangular greenness index (TGI) [46], which indicates chlorophyll content, was applied to the visual imagery at the untreated WS. Additionally, three vegetation indices (NDVI, OSAVI, and TRVI) that utilize multispectral imagery were used in estimating canopy cover at the untreated WS. Vegetation indices were calculated using the Raster Calculator function in ArcGIS, which created a raster of one band with these values.

Support vector machine (SVM) supervised classification was also used to assess canopy cover in the untreated WS. RGB imagery (red, green, and blue wavelengths) and multispectral imagery (red, green, blue, near-infrared, and red-edge wavelengths) were used for classification. Using the Training Sample Manager within ArcGIS, polygons were drawn around representative samples of juniper, bare soil, and woody debris. Training sites were selected from different areas of the image to represent the range of reflectance characteristics of each class. An initial image was created using the Interactive Supervised Classification function in order to determine how well the land cover was represented and to determine if more training samples were needed. Once each class was differentiated, the training samples were saved and used for classification. The Train Support Vector Machine Classifier tool in ArcGIS was used to create an Esri Classifier Definition (.ecd) file for each orthomosaic. Using the .ecd file, each the Classify Raster tool was used to perform classification on each raster. In order to minimize noise within the image, and remove small isolated clusters of pixels, the Majority Filter was then applied. The general supervised classification procedure used in this research is shown in Figure 2.

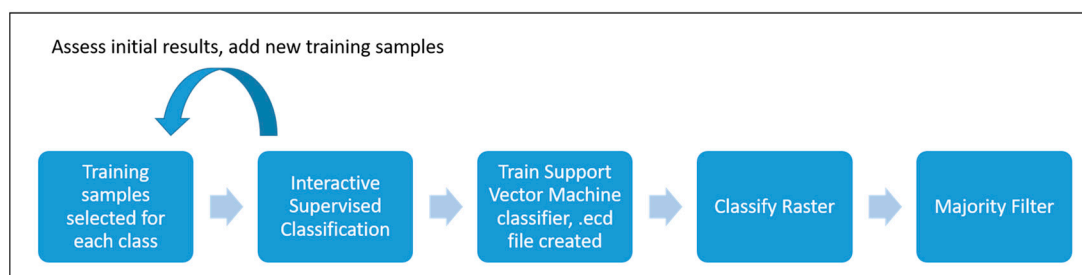


**Figure 2.** Supervised classification procedure performed in ArcMap.

A pixel-based analysis was conducted to assess juniper density and canopy cover, and total vegetation cover. By determining the number of pixels that correspond to vegetation compared to all

other types of ground cover, the percentage of vegetation and canopy cover can be estimated within a given area. For the indices selected in this research, higher values (above 0) corresponded to greater photosynthetic activity or chlorophyll depending on the index applied. For instance, values for NDVI can range from  $-1$  to  $1$ , with areas of bare soil corresponding to values of approximately  $0.025$  or less, grasslands and shrub vegetation corresponding to values of around  $0.09$ , and areas of dense vegetation corresponding to values of  $0.4$  or greater [47]. These values can vary depending on study site characteristics, vegetation type, season, sensor type and calibration, and weather conditions [48]. Based on visual inspection of the imagery (specifically examining values associated with bare ground, juniper canopy, woody debris, and shadows), threshold values were established for each index to separate vegetation from all other ground cover. The number of pixels with values greater than the threshold were divided by the total number of pixels in order to calculate the percent of canopy cover or area covered by vegetation, similar to methods described by Wu [32].

Juniper identification, juniper sapling canopy cover, and vegetation ground cover in the treated WS were assessed for two dates, July 2018 and October 2018. Support vector machine supervised classification was applied to RGB imagery, multispectral imagery (red, green, blue, NIR, and red-edge bands) and imagery with multispectral bands and NDVI values at the treated WS. The same supervised classification process described above was used in the treated WS; however, training samples in the treated WS were divided into four main categories: juniper, other vegetation, woody debris, and bare ground.

The number of pixels classified as juniper, other vegetation, bare ground, or woody debris was tabulated. Similar to calculations made for canopy cover in the untreated plots, the number of pixels represented by each class was divided by the total number of pixels to determine a percent cover of each class in the treated WS. This was then compared to estimates of juniper sapling density and vegetated ground cover calculated using the belt transect method and to the results found using line-point intercept surveys conducted in 2018 at this study site [49].

To assess the accuracy of the supervised classification in the treated WS, 249 random points were selected in each orthomosaic using the ArcGIS random point tool (one random point corresponded to a board used as a ground control point and was subsequently excluded from this analysis). Additionally, 67 pixels corresponding to juniper saplings were identified within the image and used to assess the accuracy of juniper detection specifically. For accuracy analysis, four main classes were utilized: juniper, other vegetation, woody debris, and bare ground. No assessment was made of the accuracy of detecting specific vegetation species other than western juniper. A confusion matrix was created for each orthomosaic in the treated WS. From the confusion matrix, the user's accuracy (indication of Type I error), producer's accuracy (indication of Type II error), Cohen's kappa coefficient, and overall method accuracy were calculated.

### 3. Results

#### 3.1. Ground-Based Vegetation Data Results

##### Tree Density, Height, and Canopy Cover

A greater number of juniper trees were observed in the untreated WS than in the treated WS. Based on ground counts in the two monitoring plots, average juniper tree density (of all age classes) was  $797$  trees  $\text{ha}^{-1}$  for the untreated WS. In the treated WS, juniper density was calculated to be  $313$  juniper saplings  $\text{ha}^{-1}$  based on the 41 belt transects distributed across the watershed. Mean sapling density was  $473$  trees  $\text{ha}^{-1}$  based on ground counts from the two  $2000$   $\text{m}^2$  monitoring plots at the valley and upstream locations.

The mean height of all juniper saplings surveyed in the treated WS ( $n = 113$ ) was  $0.75$  m, ranging from  $0.09$  to  $2.08$  m. Tree crown width ranged from  $0.09$  to  $1.4$  m. Data from a subsample ( $n = 18$ ) of saplings showed mean age tree was  $9$  years, ranging from  $1$  to  $15$  years. On average, saplings grew

0.1 m year<sup>-1</sup> in height and 0.04 m year<sup>-1</sup> in width. Mean sapling canopy cover was calculated to be 0.7% at the treated WS based on the belt transects.

In the untreated WS, adult trees (based on having a canopy diameter of 1.5 m or greater) made up 26% (34 of 133 trees) of all juniper at the valley monitoring plot and 16% (29 of 186 trees) of all juniper in the upstream monitoring plot. Mean sapling density was estimated to be 640 trees ha<sup>-1</sup> at the untreated WS. Tree canopy cover was 30.4% for the valley plot and 28.0% for the upstream plot in the untreated WS.

### 3.2. UAV-Based Vegetation Data Results

#### 3.2.1. Tree Canopy Cover at the Untreated Watershed (WS)

Canopy cover estimates using the UAV-based imagery at both untreated WS plots varied between vegetation indices that used visual or multispectral data (Table 3). The threshold value to determine vegetation was 0.05 for NDVI and OSAVI, 0.1 was used for TRVI and 0 was used for TGI. All pixels valued at and below the corresponding index threshold were considered to be non-vegetated areas. At the untreated WS upstream plot, NDVI, OSAVI and TRVI based estimates of canopy cover ranged from 26.1% to 27.3% (0.7% to 1.9% less than ground observations) while canopy cover measurements using TGI indicated 22.8% canopy cover (5.2% less than ground calculations). At the untreated WS valley plot, canopy cover estimates using NDVI, OSAVI, and TRVI were 33.7% to 34.5% (3.3% to 4.1% greater than ground measurements) (Figure 3). Canopy cover estimates using TGI at the untreated WS valley plot showed the largest difference from ground-based measurements at 21.2% (9.2% lower than ground estimates).

**Table 3.** Canopy cover at the untreated study plots. Method refers to the vegetation index used to calculate the canopy cover. TGI is calculated using reflectance values from the RGB (red, green, and blue bands) imagery. NDVI, OSAVI, and TRVI are calculated using reflectance values from the multispectral (red, green, blue, near-infrared, and red-edge bands) imagery. Values above the threshold value are considered vegetation. RGB classification refers to the support vector machine supervised classification performed using visual imagery. MS (multispectral bands: red, green, blue, near-infrared, and red-edge) classification refers to supervised classification performed using multispectral imagery. Ground refers to ground-based measurements of canopy cover made at each study plot.

Location	Method	Canopy Cover (%)	Threshold
Untreated WS Upstream	TGI	22.8	0
	NDVI	26.1	0.05
	OSAVI	26.7	0.05
	TRVI	27.3	0.1
	RGB classification	26.6	N/A
	MS classification	30.3	N/A
	Ground	28.0	N/A
Untreated WS Valley	TGI	21.2	0
	NDVI	33.7	0.05
	OSAVI	33.7	0.05
	TRVI	34.5	0.1
	RGB classification	29.5	N/A
	MS classification	29.4	N/A
	Ground	30.4	N/A

At the untreated WS valley site, estimates of canopy cover using SVM supervised classification (both RGB and multispectral imagery) were closer to ground-based results compared to the use of vegetation indices (Table 3). At the untreated WS upstream site, TRVI estimated canopy cover better than the SVM classification using RGB or multispectral imagery.



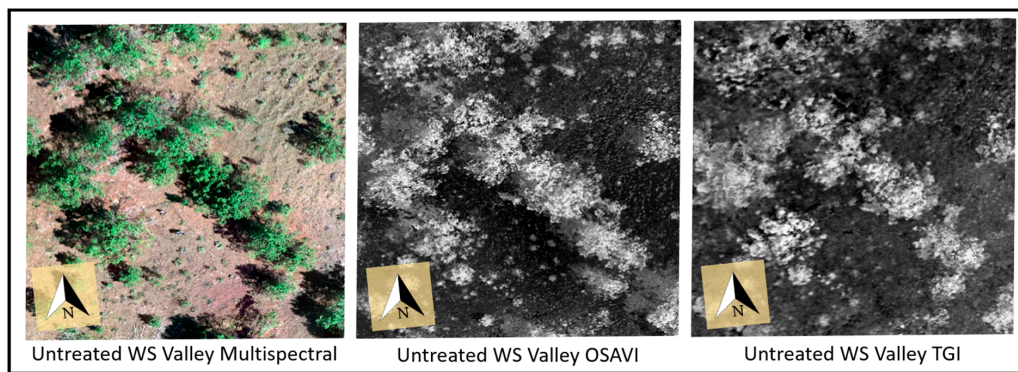


**Figure 3.** Untreated WS valley canopy cover. Darker shades correspond to lower vegetation index values and lighter shades correspond to higher values. NDVI, TRVI, and OSAVI values were similar, and therefore only OSAVI is shown for comparison. Differences can be seen in the characterization of canopy cover and in the shadows under the canopy between the OSAVI and TGI images.

### 3.2.2. Vegetation Cover and Juniper Sapling Density at the Treated WS

Based on the number of pixels corresponding to vegetation and non-vegetated areas, estimates of total vegetated ground cover based at the treated WS were similar between methods with the exception of the RGB imagery from October 2018 (Table 4). Results of these methods were also similar to line-point intercept surveys conducted in 2018 [49]. However, visual inspection of some areas of the classified rasters indicated regions where areas of bare ground and vegetation were misclassified. The use of NDVI with multispectral imagery resulted in a small difference in overall vegetated cover estimate for October imagery (0.1%) and a 1.9% difference in the estimate of vegetation cover for July imagery.

**Table 4.** Characterization of ground cover by pixel-based analysis from supervised classification from July and October 2018 at the Treated WS. RGB refers to supervised classification of RGB bands (red, green, and blue) only. Multispectral data (“MS only”) uses reflectance values from the red, green, blue, near-infrared, and red-edge wavelengths. Multispectral with NDVI (“MS+NDVI”) used the multispectral bands with the addition of NDVI values for classification. Non-vegetated ground cover refers to all other types of ground cover evaluated: bare ground and woody debris. Ground-based results are based on data collected from belt-transects and line-point transects from a study in 2018 [49].

	Juniper Cover (%)	Vegetation Cover (%)	Non-Vegetated Cover (%)
Jul 18: RGB	4.8	43.2	56.8
Jul 18: MS only	6.5	41.2	58.8
Jul 18: MS+NDVI	7.5	43.1	56.9
Oct 18: RGB	3.5	50.3	49.7
Oct 18: MS only	0.7	42.8	57.2
Oct 18: MS+NDVI	1.0	42.7	57.3
Ground	0.7	43.1	56.9

Based on the number of pixels classified as juniper, estimates of juniper sapling canopy cover using multispectral data (with and without NDVI values) from October 2018 were similar to ground-based estimates. Estimates of juniper sapling cover from multispectral imagery in July 2018 were five to six times those of the ground-based measurements. Juniper density estimates at the treated WS based on RGB imagery were 3.5% (October 2018) and 4.8% (July 2018), compared to the 0.7% juniper density calculated using belt transects.

Overall, identification of juniper saplings using supervised classification was more accurate in the October orthomosaic compared to that of imagery from July (Figure 4, Tables 5 and 6). User’s accuracy of juniper was also greater in October compared to July, regardless of the inclusion of NDVI values or if multispectral or RGB imagery was used. User’s accuracy ranged from 72.6% (RGB imagery from

July 2018) to 100% (October imagery without NDVI and October RGB imagery). Producer's accuracy for juniper ranged from 64.3% (July RGB imagery) to 88.6% (October imagery with and without NDVI). For both months, the use of NDVI resulted in slight differences in user's and producer's accuracy of juniper. The use of RGB imagery was also associated with somewhat lower producer's accuracies compared to multispectral imagery.

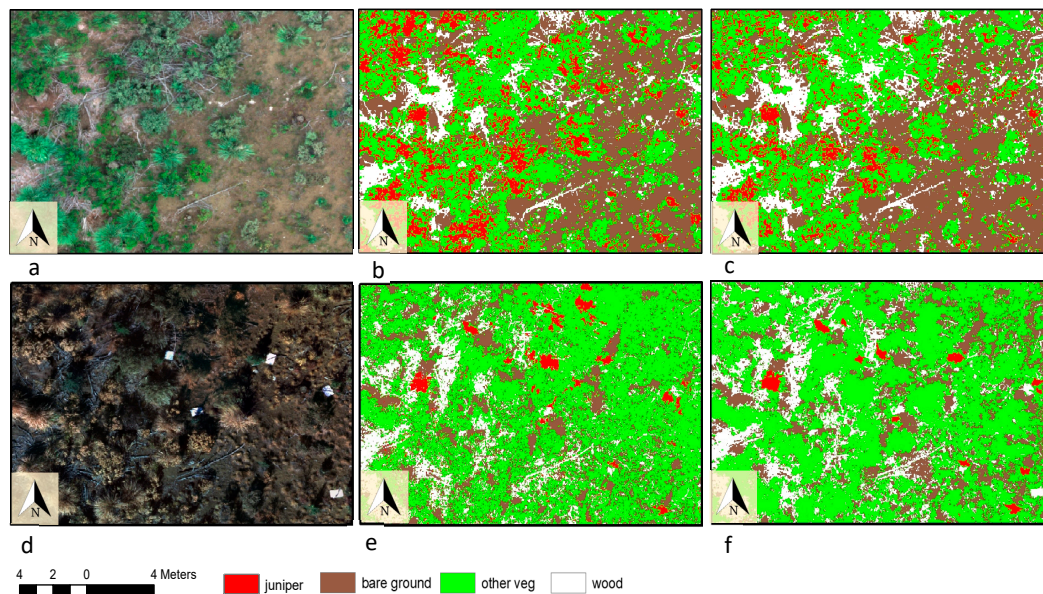


**Figure 4.** Subset of orthomosaic and classified rasters for the treated WS. July imagery is shown in top row: (a) subset of original orthomosaic, (b) classification of RGB (red, green, and blue wavelengths) raster, and (c) classification of MS (multispectral bands: red, green, blue, near-infrared, and red-edge wavelengths) without NDVI values. October imagery is displayed on the bottom row: (d) subset of original orthomosaic, (e) classification of RGB raster, and (f) classification of MS raster without NDVI. All classified images display results following the application of the Majority Filter tool. Red shading indicates pixels classified as juniper while pixels shaded green represent pixels identified as any other vegetation type. White cardboard was used to identify juniper in the October image (d) but is not present in the July image (a). “Other veg” refers to all vegetation not classified as juniper.

The accuracy of these methods to assess other types of ground cover (non-juniper vegetation, bare ground, and woody debris) was also compared (Tables 5 and 6). However, specific vegetation species other than juniper (such as sagebrush) were not analyzed for accuracy, and all pixels that corresponded to non-juniper vegetation were grouped together for analysis. Misclassification of pixels corresponding to areas of bare ground and woody debris occurred more frequently in both October orthomosaics compared to the July orthomosaics (Figure 4, Tables 5 and 6).

The overall accuracy of the supervised classification for all classes analyzed (juniper, bare ground, other vegetation, and woody debris) ranged from 76.6% (July RGB imagery) to 80.7% (July multispectral imagery with NDVI) (Table 7). The greater overall accuracy of the July orthomosaic can be largely attributed to the higher producer's accuracy of woody debris for this month. Values of Cohen's kappa coefficient for each method were similar, ranging from 0.70 to 0.74. The kappa coefficient for the juniper class only was 0.88 for both October orthomosaics, and 0.69 (multispectral imagery only) and 0.71 (multispectral imagery with NDVI) for the July orthomosaics. The use of RGB imagery resulted in very low kappa coefficients for the juniper class specifically:  $-0.08$  for RGB imagery in July and  $0.47$  for RGB imagery in October.

**Table 5.** Confusion matrix for supervised classification for July 2018, for RGB (red, green, and blue wavelengths), multispectral imagery (red, green, blue, near-infrared, and red-edge wavelengths), and multispectral imagery with NDVI values. Reference pixels are displayed by column and classified pixels are displayed by row. All vegetation that was not juniper was grouped under the class of “Other Veg”.

<b>July RGB</b>		<b>Reference</b>			
Classified	Juniper	Bare Ground	Other Veg	Wood	User’s Accuracy
Juniper	45	2	15	0	72.6
Bare Ground	0	73	3	8	86.9
Other Veg	25	6	86	0	73.5
Wood	0	8	7	38	71.7
Producer’s Accuracy	64.3	82.0	77.5	82.6	
<b>July without NDVI</b>		<b>Reference</b>			
Classified	Juniper	Bare Ground	Other Veg	Wood	User’s Accuracy
Juniper	48	1	11	0	80.0
Bare Ground	0	67	3	1	94.4
Other Veg	22	6	89	0	76.1
Wood	0	15	8	45	66.2
Producer’s Accuracy	68.6	75.3	80.2	97.8	
<b>July NDVI</b>		<b>Reference</b>			
Classified	Juniper	Bare Ground	Other Veg	Wood	User’s Accuracy
Juniper	50	1	15	0	75.8
Bare Ground	0	73	2	2	94.8
Other Veg	20	6	88	0	77.2
Wood	0	9	6	44	74.6
Producer’s Accuracy	71.4	82.0	79.3	95.7	

**Table 6.** Confusion matrix for supervised classification for October 2018, for RGB (red, green, and blue wavelengths), multispectral imagery (red, green, blue, near-infrared, and red-edge wavelengths), and multispectral imagery with NDVI values. Reference pixels are displayed by column and classified pixels are displayed by row. All vegetation that was not juniper was grouped under the class of “Other Veg”.

<b>Oct RGB</b>		<b>Reference</b>			
Classified	Juniper	Bare Ground	Other Veg	Wood	User’s Accuracy
Juniper	58	0	0	0	100.0
Bare Ground	0	67	9	5	82.7
Other Veg	11	17	76	7	68.5
Wood	1	16	7	42	63.6
Producer’s Accuracy	82.9	67.0	82.6	77.8	
<b>Oct without NDVI</b>		<b>Reference</b>			
Classified	Juniper	Bare Ground	Other Veg	Wood	User’s Accuracy
Juniper	62	0	0	0	100.0
Bare Ground	0	67	9	5	82.7
Other Veg	8	17	76	7	70.4
Wood	0	17	7	41	63.1
Producer’s Accuracy	88.6	66.3	82.6	77.4	
<b>Oct NDVI</b>		<b>Reference</b>			
Classified	Juniper	Bare Ground	Other Veg	Wood	User’s Accuracy
Juniper	62	1	0	0	98.4
Bare Ground	0	68	7	5	85.0
Other Veg	8	16	77	6	72.0
Wood	0	13	9	44	66.7
Producer’s Accuracy	88.6	69.4	82.8	80.0	

**Table 7.** Overall accuracy and Cohen’s kappa coefficient for supervised classification of each orthomosaic. Method refers to the kappa coefficient across all classes while juniper refers to the kappa coefficient only for juniper.

	Overall Accuracy (%)	Kappa (Method)	Kappa (Juniper Only)
Jul 18: RGB	76.6	0.72	−0.08
Jul 18: MS only	78.8	0.71	0.69
Jul 18: MS+NDVI	80.7	0.74	0.71
Oct 18:RGB	76.9	0.71	0.47
Oct 18: MS only	77.8	0.70	0.88
Oct 18: MS+NDVI	79.4	0.72	0.88

#### 4. Discussion

This research examined the use of ground and UAV-based techniques to assess vegetation characteristics in two watersheds, one dominated by juniper and one where the majority of juniper was removed 14 years ago. We hypothesized that the use of high-resolution UAV imagery could be used to reasonably estimate canopy cover and juniper density at this study site.

##### 4.1. Juniper Canopy Cover

Our ground-based tree canopy cover estimates (0.7% treated WS; 29.2% untreated WS) were similar to those by Ray et al. [44] who, 10 years post-treatment, estimated <1% juniper cover in the treated WS and 30% in the untreated. Our results are also similar to those by Bates et al. [50] for a similar western juniper ecosystem in southeastern Oregon; where juniper saplings occupied 0.8% of the treated plots and mature juniper occupied 29.6% of the control plots 12 years post-treatment.

Results also indicate that canopy cover estimated from vegetation indices (TRVI, NDVI, and OSAVI) derived from multispectral imagery were similar to the ground-based canopy cover estimates. Our results are similar to those by Davies et al. [51] who found a strong correlation between juniper cover estimates made using National Agriculture Imagery Program imagery and ground-based measurements using line intercepts.

Canopy cover estimates using a vegetation index (TGI) based on RGB data were not as close to our ground-based estimates when compared to those obtained using multispectral imagery. However, when supervised classification was used with RGB imagery, we found that canopy cover estimates substantially improved when compared to the use of TGI. This is similar to the findings from other studies that have successfully used RGB imagery to estimate canopy cover in other settings such as dense beech forests [26] and rice fields [52].

##### 4.2. Juniper Sapling Density and Vegetative Cover

Our ground-based estimates of juniper density (797 trees ha<sup>−1</sup>) in the untreated WS were similar to those (743 trees ha<sup>−1</sup>) reported by Fisher [43] in 2004. Supervised classification applied to multispectral imagery (with and without NDVI) collected in October 2018 produced similar estimates of juniper sapling density (0.7% and 1.0%) compared to our ground-based results (0.7%).

Several studies [24,53] have highlighted the impact of seasonal collection on the accuracy of vegetation detection. In this study, the accuracy of juniper detection in the treated WS monitoring plot was greater for October imagery when compared to July imagery. Visible differences in vegetation were apparent in the imagery collected in the fall compared to the summer, this due in part to the non-juniper vegetation had senesced or displayed reduced vigor compared to the July imagery. While data collection occurred at around the middle of the day for both flights, differences in illumination were also clear in the images. The use of RGB imagery also resulted in lower producer’s and user’s accuracies of juniper identification compared to multispectral imagery of the same month. Furthermore, low kappa coefficients of the juniper class for RGB imagery were observed during both seasons while much higher kappa coefficients for the juniper class were observed with multispectral imagery in



October. Similar to our findings, Everitt et al. [54] found differences in reflectance characteristics between juniper and surrounding vegetation during summer and spring. Juniper in northwest Texas was also found to have different reflectance characteristics than other species during the month of February but no other times of the year [55].

#### 4.3. Study Limitations and Future Research

The differences in canopy cover estimates and juniper density observed may be related to techniques and timing of data collection. While all flights were conducted around the same time of day, differences in cloud cover and topography may have influenced shading and vegetation index values. Small differences in threshold values will likely influence the canopy cover estimate and inherent differences in the ground-based measurement methods have also been found to contribute to differences in canopy cover estimates in semiarid woodlands [56]. The belt transects in the treated WS captured a wider range of topography and slopes within the watershed compared to the UAV-monitoring plot, which may not be representative of the differing vegetation characteristics.

By using small monitoring plots we were able to compare ground measurements more directly to UAV analysis to determine accuracy. However, a larger study area would encompass more topographical features of the watershed allowing us to compare results by aspect and slope. In addition to density and canopy cover, sapling height is an important characteristic in understanding juniper re-establishment. The use of UAV-based imagery to measure tree height has been demonstrated in several studies [57–59], and may provide important information regarding juniper height at this study site in future research. However, the height of juniper saplings may be similar to much of the surrounding vegetation (e.g., sagebrush) so consideration should be given to the age and structure of juniper stands.

The choice of pixel-based classification methods can influence results. A support vector machine (SVM) approach was used for supervised classification in this study. The use of SVM offers advantages over some other supervised classification methods, such as the maximum likelihood classifier, as it does not require the data to be normally distributed. However, Otukei and Blaschke [60] found that decision trees outperformed both support vector machine and maximum likelihood classifier approaches for land cover classification in open woodlands in Portugal, although all three methods produced acceptable accuracies. Another study, Joy et al. [61] successfully used decision trees to identify key vegetation types within a mixed woodland ecosystem that included pinyon-juniper species.

The accuracy of supervised classification is also dependent upon the training samples. Challenges associated with pixel-based analysis result when individual pixels may represent different classes (e.g., bare ground and wood), which may have accounted for some misclassification of wood and bare ground pixels in this study. If classes are very similar, misidentification and misclassification can occur. The use of a hybrid approach may also improve accuracy at our study site. Kumar et al. [62] found that the use of unsupervised and supervised classification together improved land cover classification in a semiarid region over using either approach alone. Additionally, in this study we used the pixel digital numbers, without radiometric calibration, for analysis. While imagery was visually assessed, in order to assess temporal changes or fuse imagery from multiple dates together, radiometric corrections should be made in future research.

This study utilized pixel-based image analysis based on pixel brightness values. Future research utilizing object-based image analysis (OBIA) incorporating shape and texture into classification may help delineate between juniper and other vegetation species. Baena et al. [63] found that OBIA, when used in combination with structure from motion (SfM) derived height models, could be used to assess the density of tree species in Northern Peru. While the ArcGIS Majority Filter tool was used in this research to minimize isolated pixels, the use of OBIA has been shown to reduce the amount of scattered pixels in high-resolution imagery [64].

The results of this study demonstrated the potential use of quadcopter UAV for evaluating juniper canopy cover and density, when seasonal limitations for data collection are considered. As in



Breckenridge et al. [65], our vegetative cover measurements using UAV-based multispectral imagery were similar to ground-based measurements. However, the accuracy of juniper sapling identification varied between seasons. Similar to the results found by Tay et al. [39], we found that pixel-based classification applied to UAV images can accurately detect and monitor vegetation. Given the large scale of juniper expansion and time requirements associated with ground surveys, the use of UAV offers the advantage of more efficient data collection compared to using ground-based techniques alone. UAV also offer a high-resolution, flexible platform which can be used by land managers to target specific study sites, times, and objectives.

Our study was specifically designed to evaluate UAV techniques for the management of juniper ecosystems. Similar to research by Lehmann et al. [66], future research at this study site includes expanding the techniques used in this study to characterize the spatial distribution of invasive species such as cheatgrass, which negatively affect rangeland ecosystems in the Pacific Northwest. A variety of other UAV applications such as in forest conservation planning, post-fire recovery, and estimation of dendrometric parameters for timber extraction forecast will likely become more common in the near future [67] because of the high cost, time and labor involved in traditional extensive field methods, especially in inaccessible locations [68].

## 5. Conclusions

This study evaluated western juniper canopy cover and density in a treated (juniper removed) and an untreated WS using ground-based and UAV-based methods. This research found that, as expected, juniper canopy cover and density were greater at the untreated WS compared to the treated WS. When supervised classification or multispectral vegetation indices were used, estimates of mature juniper canopy cover were similar to ground-based results. Additionally, we found that juniper sapling reestablishment post-treatment was of similar magnitude to that obtained in previous studies by different methods in the same ecosystem.

The results of this study also emphasize the importance of considering the seasonal characteristics of vegetation when collecting data. Juniper identification was more accurately achieved with October multispectral imagery than with July multispectral imagery or with RGB imagery. However, estimates of vegetation cover in the treated WS were similar, with the exception of RGB imagery from October, to ground-based estimates regardless of the season of collection. Although specific objectives and data collection regimes should be considered, UAV techniques are promising tools for monitoring western juniper expansion and monitoring vegetation cover in semiarid ecosystems.

**Author Contributions:** N.D. and C.G.O. developed the study design and conducted field data collection and analyses. R.M.-G. provided expert knowledge used in data analysis and interpretation. All co-authors contributed to the writing of the manuscript.

**Funding:** This study was funded in part by the Oregon Beef Council, Oregon Watershed Enhancement Board, USDA NIFA, and the Oregon Agricultural Experiment Station.

**Acknowledgments:** The authors gratefully acknowledge the continuous support of the Hatfield High Desert Ranch, the U.S. Department of Interior Bureau of Land Management—Prineville Office, and the OSU's Extension Service, in this research effort. Our thanks go to Tim Deboodt, Michael Fisher, and John Buckhouse for paving the road for this important long-term study. Also, we want to thank the multiple other graduate and undergraduate students from Oregon State University, and volunteers, who participated in various field data collection activities related to the results here presented.

**Conflicts of Interest:** The authors declare no conflict of interest.

## References

1. Miller, R.F.; Tausch, R.J.; McAArthur, E.D.; Johnson, D.D.; Sanderson, S.C. *Age Structure and Expansion of Pinon-Juniper Woodlands: A Regional Perspective in the Intermountain West*; Research Paper RMRS-RP-69; U.S. Department of Agriculture, Forest Service: Fort Collins, CO, USA, 2008.
2. Miller, R.F.; Bates, J.D.; Svejcar, T.J.; Pierson, F.B.; Eddleman, L.E. *Biology, Ecology, and Management of Western Juniper (Juniperus occidentalis)*; Oregon State University, Agricultural Experiment Station: Corvallis, OR, USA, 2005; Volume 152.
3. Caracciolo, D.; Istanbuloglu, E.; Noto, L.V. An ecohydrological cellular automata model investigation of juniper tree encroachment in a western North American landscape. *Ecosystems* **2017**, *20*, 1104–1123. [[CrossRef](#)]
4. Waichler, W.S.; Miller, R.F.; Doescher, P.S. Community characteristics of old-growth western juniper woodlands. *J. Range Manag.* **2001**, *54*, 518–527. [[CrossRef](#)]
5. Miller, R.F.; Rose, J.A. Historic expansion of *Juniperus occidentalis* (western juniper) in southeastern Oregon. *Gt. Basin Nat.* **1995**, *55*, 37–45.
6. Coultrap, D.E.; Fulgham, K.O.; Lancaster, D.L.; Gustafson, J.; Lile, D.F.; George, M.R. Relationships between western juniper (*Juniperus occidentalis*) and understory vegetation. *Invasive Plant Sci. Manag.* **2008**, *1*, 3–11. [[CrossRef](#)]
7. Miller, R.F.; Svejcar, T.J.; Rose, J.A. Impacts of western juniper on plant community composition and structure. *J. Range Manag.* **2000**, *53*, 574–585. [[CrossRef](#)]
8. Lebron, I.; Madsen, M.D.; Chandler, D.G.; Robinson, D.A.; Wendroth, O.; Belnap, J. Ecohydrological controls on soil moisture and hydraulic conductivity within a pinyon-juniper woodland. *Water Resour. Res.* **2007**, *43*, W08422. [[CrossRef](#)]
9. Mollnau, C.; Newton, M.; Stringham, T. Soil water dynamics and water use in a western juniper (*Juniperus occidentalis*) woodland. *J. Arid Environ.* **2014**, *102*, 117–126. [[CrossRef](#)]
10. Pierson, F.B.; Williams, C.J.; Hardegree, S.P.; Clark, P.E.; Kormos, P.R.; Al-Hamdan, O.Z. Hydrologic and erosion responses of sagebrush steppe following juniper encroachment, wildfire, and tree cutting. *Rangel. Ecol. Manag.* **2013**, *66*, 274–289. [[CrossRef](#)]
11. Dittel, J.W.; Sanchez, D.; Ellsworth, L.M.; Morozumi, C.N.; Mata-Gonzalez, R. Vegetation response to juniper reduction and grazing exclusion in sagebrush-steppe habitat in eastern Oregon. *Rangel. Ecol. Manag.* **2018**, *71*, 213–219. [[CrossRef](#)]
12. Reid, K.; Wilcox, B.; Breshears, D.; Macdonald, L. Runoff and erosion in a pinon-juniper woodland: Influence of vegetation patches. *Soil Sci. Soc. Am. J.* **1999**, *63*, 1869–1879. [[CrossRef](#)]
13. Pierson, F.B.; Bates, J.D.; Svejcar, T.J.; Hardegree, S.P. Runoff and erosion after cutting western juniper. *Rangel. Ecol. Manag.* **2007**, *60*, 285–292. [[CrossRef](#)]
14. Petersen, S.L.; Stringham, T.K. Infiltration, runoff, and sediment yield in response to western juniper encroachment in southeast Oregon. *Rangel. Ecol. Manag.* **2008**, *61*, 74–81. [[CrossRef](#)]
15. O'Connor, C.; Miller, R.; Bates, J.D. Vegetation response to western juniper slash treatments. *Environ. Manag.* **2013**, *52*, 553–566. [[CrossRef](#)] [[PubMed](#)]
16. Pierson, F.B.; Williams, C.J.; Kormos, P.R.; Hardegree, S.P.; Clark, P.E.; Rau, B.M. Hydrologic vulnerability of sagebrush steppe following pinyon and juniper encroachment. *Rangel. Ecol. Manag.* **2010**, *63*, 614–629. [[CrossRef](#)]
17. Sankey, T.T.; Glenn, N.; Ehinger, S.; Boehm, A.; Hardegree, S. Characterizing western juniper expansion via a fusion of Landsat 5 Thematic mapper and lidar data. *Rangel. Ecol. Manag.* **2010**, *63*, 514–523. [[CrossRef](#)]
18. Petersen, S.L.; Stringham, T.K. Development of GIS-based models to predict plant community structure in relation to western juniper establishment. *For. Ecol. Manag.* **2008**, *256*, 981–989. [[CrossRef](#)]
19. Roundy, D.B.; Hulet, A.; Roundy, B.A.; Jensen, R.R.; Hinkle, J.B.; Crook, L.; Petersen, S.L. Estimating pinyon and juniper cover across Utah using NAIP imagery. *Environment* **2016**, *3*, 765–777. [[CrossRef](#)]
20. Yang, J.; Weisberg, P.J.; Bristow, N.A. Landsat remote sensing approaches for monitoring long-term tree cover dynamics in semi-arid woodlands: Comparison of vegetation indices and spectral mixture analysis. *Remote Sens. Environ.* **2012**, *119*, 62–71. [[CrossRef](#)]

21. Meddens, A.J.H.; Hicke, J.A.; Jacobs, B.F. Characterizing the response of piñon-juniper woodlands to mechanical restoration using high-resolution satellite imagery. *Rangel. Ecol. Manag.* **2016**, *69*, 215–223. [[CrossRef](#)]
22. Xian, G.; Homer, C.; Aldridge, C. Assessing long-term variations in sagebrush habitat—Characterization of spatial extents and distribution patterns using multi-temporal satellite remote-sensing data. *Int. J. Remote Sens.* **2012**, *33*, 2034–2058. [[CrossRef](#)]
23. Howell, R.G.; Petersen, S.L. A comparison of change detection measurements using object-based and pixel-based classification methods on western juniper dominated woodlands in eastern Oregon. *AIMS Environ. Sci.* **2017**, *4*, 348–357. [[CrossRef](#)]
24. Lu, B.; He, Y. Species classification using Unmanned Aerial Vehicle (UAV)-acquired high spatial resolution imagery in a heterogeneous grassland. *ISPRS J. Photogramm. Remote Sens.* **2017**, *128*, 73–85. [[CrossRef](#)]
25. D'Oleire-Oltmanns, S.; Marzloff, I.; Peter, K.D.; Ries, J.B. Unmanned aerial vehicle (UAV) for monitoring soil erosion in Morocco. *Remote Sens.* **2012**, *4*, 3390–3416. [[CrossRef](#)]
26. Chianucci, F.; Disperati, L.; Guzzi, D.; Bianchini, D.; Nardino, V.; Lastri, C.; Rindinella, A.; Corona, P. Estimation of canopy attributes in beech forests using true colour digital images from a small fixed-wing UAV. *Int. J. Appl. Earth Obs. Geoinform.* **2016**, *47*, 60–68. [[CrossRef](#)]
27. Carreiras, J.M.B.; Pereira, J.M.C.; Pereira, J.S. Estimation of tree canopy cover in evergreen oak woodlands using remote sensing. *For. Ecol. Manag.* **2006**, *223*, 45–53. [[CrossRef](#)]
28. Krofcheck, D.J.; Eitel, J.U.H.; Lippitt, C.D.; Vierling, L.A.; Schulthess, U.; Litvak, M.E. Remote sensing based simple models of GPP in both disturbed and undisturbed piñon-juniper woodlands in the southwestern U.S. *Remote Sens.* **2016**, *8*, 20. [[CrossRef](#)]
29. Zhou, X.; Zheng, H.B.; Xu, X.Q.; He, J.Y.; Ge, X.K.; Yao, X.; Cheng, T.; Zhu, Y.; Cao, W.X.; Tian, Y.C. Predicting grain yield in rice using multi-temporal vegetation indices from UAV-based multispectral and digital imagery. *ISPRS J. Photogramm. Remote Sens.* **2017**, *130*, 246–255. [[CrossRef](#)]
30. Akar, A.; Gökalp, E.; Akar, Ö.; Yilmaz, V. Improving classification accuracy of spectrally similar land covers in the rangeland and plateau areas with a combination of worldview-2 and UAV images. *Geocarto Int.* **2017**, *32*, 990–1003. [[CrossRef](#)]
31. Rouse, J.W.; Harlan, J.C.; Haas, R.H.; Schell, J.A.; Deering, D.W. *Monitoring the Vernal Advancement and Retrogradation (Green Wave Effect) of Natural Vegetation*; Texas A&M University, Remote Sensing Center: College Station, TX, USA, 1974.
32. Wu, W. Derivation of tree canopy cover by multiscale remote sensing approach. *Int. Arch. Photogramm.* **2011**, *142–149*. [[CrossRef](#)]
33. Rondeaux, G.; Steven, M.; Baret, F. Optimization of soil-adjusted vegetation indices. *Remote Sens. Environ.* **1996**, *55*, 95–107. [[CrossRef](#)]
34. Fadaei, H.; Suzuki, R.; Sakaic, T.; Toriid, K. A Proposed new vegetation index, the total ratio vegetation index (TRVI), for arid and semiarid regions. *ISPRS Int. Arch. Photogramm. Remote Sens. Spat. Inf. Sci.* **2012**, *1*, 403–407. [[CrossRef](#)]
35. Akkermans, T.; Van Rompaey, A.; Van Lipzig, N.; Moonen, P.; Verbist, B. Quantifying successional land cover after clearing of tropical rainforest along forest frontiers in the Congo Basin. *Phys. Geogr.* **2013**, *34*, 417–440. [[CrossRef](#)]
36. Koppad, A.G.; Janagoudar, B.S. Vegetation analysis and land use land cover classification of forest in Uttara Kannada District India using remote sensing and GIS techniques. *ISPRS Int. Arch. Photogramm. Remote Sens. Spat. Inf. Sci.* **2017**, *XLII-4/W5c*, 121–125. [[CrossRef](#)]
37. García-Romero, L.; Hernández-Cordero, A.I.; Hernández-Calvento, L.; Espino, E.P.; López-Valcarcel, B.G. Procedure to automate the classification and mapping of the vegetation density in arid aeolian sedimentary systems. *Prog. Phys. Geogr. Earth Environ.* **2018**, *42*, 330–351. [[CrossRef](#)]
38. Papadopoulos, A.V.; Kati, V.; Chachalis, D.; Kotoulas, V.; Stamatiadis, S. Weed mapping in cotton using ground-based sensors and GIS. *Environ. Monit. Assess.* **2018**, *190*, 622. [[CrossRef](#)]
39. Tay, J.Y.L.; Erfmeier, A.; Kalwij, J.M. Reaching new heights: Can drones replace current methods to study plant population dynamics? *Plant Ecol.* **2018**, *219*, 1139–1150. [[CrossRef](#)]
40. Bauer, T.; Strauss, P. A rule-based image analysis approach for calculating residues and vegetation cover under field conditions. *Catena* **2014**, *113*, 363–369. [[CrossRef](#)]

41. Ochoa, C.G.; Caruso, P.; Ray, G.; Deboodt, T.; Jarvis, W.T.; Guldán, S.J. Ecohydrologic connections in semiarid watershed systems of central Oregon USA. *Water* **2018**, *10*, 181. [[CrossRef](#)]
42. Deboodt, T.L. Watershed Response to Western Juniper Control. Ph.D. Dissertation, Oregon State University, Corvallis, OR, USA, 2008.
43. Fisher, M. Analysis of Hydrology and Erosion in Small, Paired Watersheds in a Juniper-Sagebrush Area of Central Oregon. Ph.D. Dissertation, Oregon State University, Corvallis, OR, USA, 2004.
44. Ray, G.; Ochoa, C.G.; Deboodt, T.; Mata-Gonzalez, R. Overstory–understory vegetation cover and soil water content observations in western juniper woodlands: A paired watershed study in Central Oregon, USA. *Forests* **2019**, *10*, 151. [[CrossRef](#)]
45. Phipps, R.L. *Collecting, Preparing, Crossdating, and Measuring Tree Increment Cores*; US Department of the Interior, Geological Survey: Washington, DC, USA, 1985.
46. Hunt, E.R.; Doraiswamy, P.C.; McMurtrey, J.E.; Daughtry, C.S.T.; Perry, E.M.; Akhmedov, B. A visible band index for remote sensing leaf chlorophyll content at the canopy scale. *Int. J. Appl. Earth Obs. Geoinform.* **2013**, *21*, 103–112. [[CrossRef](#)]
47. Holben, B.N. Characteristics of maximum-value composite images from temporal AVHRR data. *Int. J. Remote Sens.* **1986**, *7*, 1417–1434. [[CrossRef](#)]
48. Wang, R.; Gamon, J.A.; Montgomery, R.A.; Townsend, P.A.; Zyguelbaum, A.I.; Bitan, K.; Tilman, D.; Cavender-Bares, J. Seasonal variation in the NDVI–species richness relationship in a prairie grassland experiment (Cedar Creek). *Remote Sens.* **2016**, *8*, 128. [[CrossRef](#)]
49. Durfee, N. Ecohydrologic Connections in Semiarid Rangeland Ecosystems in Oregon. Master’s Thesis, Oregon State University, Corvallis, OR, USA, 2018.
50. Bates, J.D.; Svejcar, T.; Miller, R.; Davies, K.W. Plant community dynamics 25 years after juniper control. *Rangel. Ecol. Manag.* **2017**, *70*, 356–362. [[CrossRef](#)]
51. Davies, K.W.; Petersen, S.L.; Johnson, D.D.; Davis, D.B.; Madsen, M.D.; Zvirzdin, D.L.; Bates, J.D. Estimating juniper cover From National Agriculture Imagery Program (NAIP) imagery and evaluating relationships between potential cover and environmental variables. *Rangel. Ecol. Manag. Lawrence* **2010**, *63*, 630–637. [[CrossRef](#)]
52. Lee, K.J.; Lee, B.W. Estimating canopy cover from color digital camera image of rice field. *J. Crop Sci. Biotechnol.* **2011**, *14*, 151–155. [[CrossRef](#)]
53. Ahmadpour, A.; Shokri, M.; Solaimani, K.; Ghorbani, J. Evaluation of satellite data efficiency in identification of plant groups. *Acta Ecol. Sin.* **2011**, *31*, 303–309. [[CrossRef](#)]
54. Everitt, J.H.; Yang, C.; Johnson, H.B. Canopy spectra and remote sensing of ashe juniper and associated vegetation. *Environ. Monit. Assess.* **2007**, *130*, 403–413. [[CrossRef](#)]
55. Everitt, J.H.; Yang, C.; Racher, B.J.; Britton, C.M.; Davis, M.R. Remote sensing of redberry juniper in the Texas rolling plains. *J. Range Manag.* **2001**, *54*, 254–259. [[CrossRef](#)]
56. Ko, D.; Bristow, N.; Greenwood, D.; Weisberg, P. Canopy cover estimation in semiarid woodlands: Comparison of field-based and remote sensing methods. *For. Sci.* **2009**, *55*, 10.
57. Birdal, A.C.; Avdan, U.; Türk, T. Estimating tree heights with images from an unmanned aerial vehicle. *Geomat. Nat. Hazards Risk* **2017**, *8*, 1144–1156. [[CrossRef](#)]
58. Wallace, L.; Lucieer, A.; Malenovsky, Z.; Turner, D.; Vopenka, P. Assessment of forest structure using two UAV techniques: A comparison of airborne Laser scanning and structure from motion (sfm) point clouds. *Forests* **2016**, *7*, 62. [[CrossRef](#)]
59. Panagiotidis, D.; Abdollahnejad, A.; Surový, P.; Chiteculo, V. Determining tree height and crown diameter from high-resolution UAV imagery. *Int. J. Remote Sens.* **2017**, *38*, 2392–2410. [[CrossRef](#)]
60. Otukey, J.R.; Blaschke, T. Land cover change assessment using decision trees, support vector machines and maximum likelihood classification algorithms. *Int. J. Appl. Earth Obs. Geoinf.* **2010**, *12*, S27–S31. [[CrossRef](#)]
61. Joy, S.M.; Reich, R.M.; Reynolds, R.T. A non-parametric, supervised classification of vegetation types on the Kaibab National Forest using decision trees. *Int. J. Remote Sens.* **2003**, *24*, 1835–1852. [[CrossRef](#)]
62. Kumar, P.; Singh, B.K.; Rani, M. An efficient hybrid classification Approach for land use/land cover analysis in a semi-desert area using ETM+ and LISS-III sensor. *IEEE Sens. J.* **2013**, *13*, 2161–2165. [[CrossRef](#)]
63. Baena, S.; Moat, J.; Whaley, O.; Boyd, D.S. Identifying species from the air: UAVs and the very high resolution challenge for plant conservation. *PLoS ONE* **2017**, *12*, e0188714. [[CrossRef](#)]

64. Laliberte, A.S.; Rango, A.; Herrick, J.E.; Fredrickson, E.L.; Burkett, L. An object-based image analysis approach for determining fractional cover of senescent and green vegetation with digital plot photography. *J. Arid Environ.* **2007**, *69*, 1–14. [[CrossRef](#)]
65. Breckenridge, R.P.; Dakins, M.; Bunting, S.; Harbour, J.L.; Lee, R.D. Using unmanned helicopters to assess vegetation cover in sagebrush steppe ecosystems. *Rangel. Ecol. Manag.* **2012**, *65*, 362–370. [[CrossRef](#)]
66. Lehmann, J.R.K.; Prinz, T.; Ziller, S.R.; Thiele, J.; Heringer, G.; Meira-Neto, J.A.A.; Buttschardt, T.K. Open-source processing and analysis of aerial imagery acquired with a low-cost unmanned aerial system to support invasive plant management. *Front. Environ. Sci.* **2017**, *5*, 44. [[CrossRef](#)]
67. Torresan, C.; Berton, A.; Carotenuto, F.; Gennaro, S.F.D.; Gioli, B.; Matese, A.; Miglietta, F.; Vagnoli, C.; Zaldei, A.; Wallace, L. Forestry applications of UAVs in Europe: A review. *Int. J. Remote Sens.* **2017**, *38*, 2427–2447. [[CrossRef](#)]
68. Martínez-Salvador, M.; Mata-Gonzalez, R.; Pinedo-Alvarez, A.; Morales-Nieto, C.R.; Prieto-Amparán, J.A.; Vázquez-Quintero, G.; Villarreal-Guerrero, F. A spatial forestry productivity potential model for *pinus arizonica engelm*, a key timber species from Northwest Mexico. *Sustainability* **2019**, *11*, 829. [[CrossRef](#)]



© 2019 by the authors. Licensee MDPI, Basel, Switzerland. This article is an open access article distributed under the terms and conditions of the Creative Commons Attribution (CC BY) license (<http://creativecommons.org/licenses/by/4.0/>).